BIOCHEMISTRY
including biophysical chemistry & molecular biology

Article

pubs.acs.org/biochemistry

Involvement of the β3-α3 Loop of the Proline Dehydrogenase Domain in Allosteric Regulation of Membrane Association of Proline Utilization A

Weidong Zhu,[§] Ashley M. Haile,[§] Ranjan K. Singh,[∥] John D. Larson,[∥] Danielle Smithen,[§] Jie Y. Chan,[§] John J. Tanner,[∥,⊥] and Donald F. Becker*[,§]

[§]Department of Biochemistry, Redox Biology Center, University of Nebraska-Lincoln, Lincoln, Nebraska 68588, United States
[∥]Departments of Chemistry and [⊥]Biochemistry, University of Missouri-Columbia, Columbia, Missouri 65211, United States

Supporting Information

ABSTRACT: Proline utilization A (PutA) from *Escherichia coli* is a membrane-associated trifunctional flavoenzyme that catalyzes the oxidation of proline to glutamate and moonlights as a transcriptional regulator. As a regulatory protein, PutA represses transcription of the *put* regulon, which contains the genes encoding PutA and the proline transporter PutP. The binding of proline to the proline dehydrogenase active site and the subsequent reduction of the flavin induce high affinity membrane association of PutA and relieve repression of the *put* regulon, thereby causing PutA to switch from its regulatory to its enzymatic role. Here, we present evidence suggesting that residues of the β3-α3 loop of the proline dehydrogenase domain $(\beta\alpha)_8$ barrel are involved in proline-mediated allosteric regulation of PutA-membrane binding. Mutation of the conserved residues Asp370 and Glu372 in the β3-α3 loop abrogates the ability of proline to induce functional membrane association. Both *in vitro* lipid/membrane binding assays and *in vivo* cell-based assays demonstrate that mutagenesis of Asp370 (D370N/A) or Glu372 (E372A) dramatically impedes PutA functional switching. The crystal structures of the proline dehydrogenase domain mutants PutA86−630D370N and PutA86−630D370A complexed with the proline analogue L-tetrahydro-2-furoic acid show that the mutations cause only minor perturbations to the active site but no major structural changes, suggesting that the lack of proline response is not due to a failure of the mutated active sites to correctly bind the substrate. Rather, these results suggest that the β3-α3 loop may be involved in transmitting the status of the proline dehydrogenase active site and flavin redox state to the distal membrane association domain.

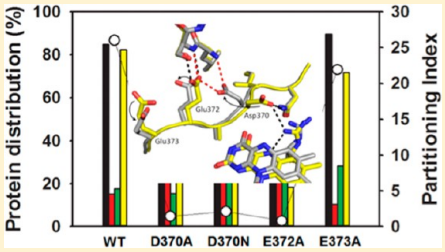

Proline utilization A (PutA) proteins are bifunctional membrane-associated enzymes found in Gram-negative bacteria that catalyze the 4-electron oxidation of proline to glutamate (Scheme 1).[1,2] PutAs have two distinct enzyme active sites.[1] The proline dehydrogenase (PRODH) site contains a noncovalently bound flavin adenine dinucleotide (FAD) cofactor and catalyzes the oxidation of proline to Δ^1-pyrroline-5-carboxylate (P5C).[3] The P5C dehydrogenase (P5CDH) site catalyzes the NAD^+-dependent oxidation of γ-glutamate semialdehyde (GSA) to glutamate using a catalytic cysteine. The equilibrium between P5C and GSA involves the hydrolysis of the former species and links the two enzyme-catalyzed reactions (Scheme 1).

Some PutAs moonlight as autogenous transcriptional repressors. PutA from *Escherichia coli* (EcPutA) is the archetype of moonlighting PutAs, which are also called "trifunctional" PutAs in reference to their PRODH, P5CDH, and regulatory functions.[1] Whether such PutAs perform their enzymatic or repressor roles depends on the availability of proline in the environment. When proline levels are low, PutA binds to the 419-bp *put* control DNA region that separates the divergently transcribed genes encoding PutA and the proline transporter PutP.[4] This protein−DNA interaction, which is mediated by the N-terminal ribbon−helix−helix DNA-binding domain, represses transcription of the *put* regulon genes.[4] When sufficient levels of proline are present in the bacterium's environment, repression of the *put* genes is relieved, and PutA is localized to the inner membrane where it catalyzes the reactions shown in Scheme 1.[4,5]

Although the mechanism by which proline induces tight PutA-membrane binding remains an outstanding question, there is a consensus that the occupancy of the PRODH active site and the redox state of the FAD are the primary determinants of whether EcPutA functions as a DNA-bound repressor or a membrane-associated enzyme.[6−8] We have shown that reduction of the FAD has a dramatic effect on membrane binding[5,9] but a negligible effect on DNA binding.[9] Surface plasmon resonance studies have shown that oxidized PutA displays no binding to *E. coli* polar lipid vesicles, the binding of the nonreducing proline analogue L-tetrahydro-2-furoic acid (THFA) to PutA stimulates moderately high binding (K_D = 34 nM), and the proline-reduced enzyme

Received: March 27, 2013
Revised: May 24, 2013
Published: May 28, 2013

   dx.doi.org/10.1021/bi400396g | *Biochemistry* 2013, 52, 4482−4491

Scheme 1

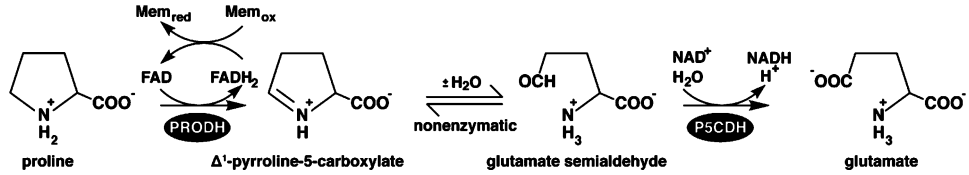

exhibits very tight binding with a dissociation constant below 0.01 nM.[5] Furthermore, we have shown that reduction of the flavin causes changes in the limited proteolysis patterns of PutA, implying that flavin reduction induces global conformational changes.[10] Taken together, these results suggest that proline is an allosteric effector of membrane binding.

Information about the conformational changes in the PRODH active site involved in allosteric regulation of membrane binding emerged recently from a study of the mechanism-based inactivation of EcPutA by *N*-propargylglycine (PPG).[11] Spectroscopic, membrane association, and limited proteolysis data suggest that inactivation by PPG locks EcPutA into a conformation that closely resembles the proline reduced, membrane-associated form of the enzyme.[11] The crystal structure of the EcPutA PRODH domain (residues 86−630, PutA86−630) inactivated by PPG suggests that flavin reduction induces dramatic rearrangement of the FAD ribityl chain, severe bending of the isoalloxazine ring, and rupture of an electrostatic network linking the FAD N(5) atom, Arg431, and Asp370. Involvement of the ribityl chain, N(5), and Arg431 in functional switching of EcPutA is also supported by previous biochemical studies of EcPutA.[8] The FAD (N5) and Arg431 interaction was shown to be pivotal for triggering functional switching of EcPutA.[8] It is unclear, however, how signals are transmitted beyond this critical juncture. The involvement of Asp370 in functional switching has not yet been investigated.

It is interesting to note that Asp370 is identically conserved among PutAs,[12] and previous structures of the EcPutA PRODH domain[13,14] have shown that this residue is located in the loop connecting β3 and α3 of the $(\beta\alpha)_8$ barrel (Figure 1A). In the crystal structure of the PRODH domain complexed with THFA, Asp370 forms several noncovalent interactions not only with Arg431, but with other active site residues Tyr540, Lys329, and Asn368. The structure of PPG-inactivated PutA86−630 suggests that reduction of the FAD breaks these interactions, causing Asp370 to rotate 180° away from Arg431 and toward two conserved glutamate residues also located on the β3-α3 loop, Glu372 and Glu373 (Figure 1B).[11] Motivated by the observation of this redox-linked conformational change of Asp370, and the high conservation of residues in the β3-α3 loop, we used a mutagenesis approach to investigate the possible involvement of Asp370, Glu372, and Glu373 in the regulation of PutA-membrane binding.

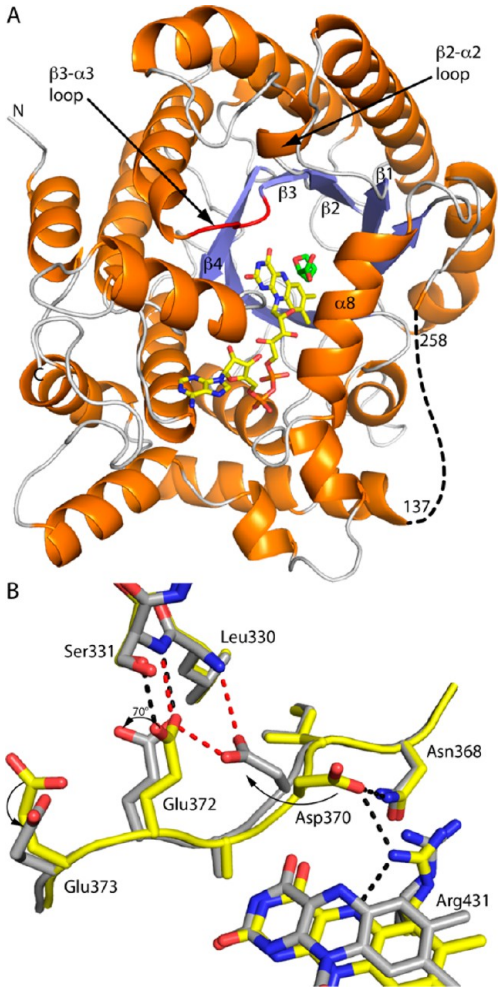

Figure 1. (A) Ribbon representation of PutA86−630 complexed with THFA. The $(\beta\alpha)_8$ barrel is shown with the β3-α3 loop colored red, FAD yellow, and THFA green. (B) Structural overlay of the β3-α3 loop regions of PutA86−630-THFA (yellow, PDB 1TIW) and PPG-inactivated PutA86−630 (gray, PDB 3ITG). Black and red dashed lines represent electrostatic interactions in PutA86−630−THFA and PPG-inactivated PutA86−630, respectively. The arrows denote conformational changes induced by enzyme inactivation. This figure and others were prepared using PyMol.[30]

EXPERIMENTAL PROCEDURES

Mutagenesis and Protein Purification. Site-directed mutants were made from the full-length construct of wild-type *E. coli* PutA (PutA-pET14b) and the proline dehydrogenase domain construct PutA86−630 (PutA86−630-pET14b) using the Stratagene QuikChange mutagenesis kit. Oligonucleotides used for mutagenesis were D370A, 5′-GATATTGGTATCAACATTGCCGCCGA-3′; D370N, 5′-GGTATCAACATTAACGCCGAAGAGTG-3′; E372A, 5′-TCAACATTGACGCCGCAGAGTCCGATCGCCT-3; and E373A, 5′-TCCAGGCGATCGGACGCTTCGGCGTCAATG-3′. PutA wild-type and mutant proteins were overexpressed in *E. coli* and purified by Ni-NTA affinity chromatography using a N-terminal His-tag as described previously for wild-type PutA.[8] The His-tag was retained in the subsequent experiments. The amount of bound FAD in the purified PutA mutants was determined as previously described.[9] The concentrations of the PutA proteins were determined from the amount of FAD bound to normalize for differences in FAD content.

PRODH Kinetic Assays. The kinetic parameters of PRODH activity for PutA wild-type and mutants D370A,

dx.doi.org/10.1021/bi400396g | *Biochemistry* 2013, 52, 4482−4491

D370N, E372A, and E373A were determined at 23 °C by varying proline concentration (0−1.6 M). The effect of pH on PRODH activity was determined from pH 6.0 to 9.5 using a mixed buffer system comprising 20 mM each of 2-(*N*-morpholino)ethanesulfonic acid, 3-(*N*-morpholino)-propanesulfonic acid (MOPS), *N*-(2-hydroxyethyl)piperazine-*N*′-2-ethanesulfonic acid (HEPES), *N*-tris(hydroxymethyl)-4-aminobutanesulfonic acid, and *N*-cyclohexyl-2-aminoethanesulfonic acid. Proline stock solutions (3 M) were adjusted with NaOH to the corresponding pH values of the assays. PRODH activity was measured using dichlorophenolindophenol (DCPIP) as the terminal electron acceptor and phenazine methosulfate as the mediator (proline/DCPIP oxidoreductase assay) as previously described.[8,9] One unit of PRODH activity is the quantity of enzyme that transfers electrons from 1 μmol of proline to DCPIP per min at 23 °C. Assays were performed in triplicate and values for K_m and k_{cat} were estimated by nonlinear regression to the Michaelis−Menten equation (Table 1). Also, control assays with high concentrations of NaCl (>1 M) in the assay buffer showed that PRODH activity is not affected by changes in ionic strength at high proline concentrations.

Table 1. Kinetic Parameters[a] and Redox Potentials[b] of PutA Mutants

PutA	k_{cat} (s^{-1}) (pK_a)	K_m (M) (pK_a)	k_{cat}/K_m (s^{-1} M^{-1}) (pK_a)	E_m (mV)
wild-type	6.75 ± 0.11 (7.3 ± 0.2)	0.23 ± 0.02 (7.2 ± 0.5)	29.5 ± 0.4 (7.4 ± 0.2)	−106
D370A	3.48 ± 0.25 (7.5 ± 0.1)	1.81 ± 0.21 (8.5 ± 0.2)	1.9 ± 0.4 (8.8 ± 0.3)	−81
D370N	1.87 ± 0.22 (ND)	0.65 ± 0.04 (ND)	2.9 ± 0.5 (ND)	−82
E372A	3.34 ± 0.30 (8.1 ± 0.2)	0.56 ± 0.09 (7.3 ± 0.4)	6.0 ± 0.3 (8.1 ± 0.1)	−103
E373A	7.29 ± 0.18 (6.8 ± 0.3)	0.38 ± 0.05 (7.5 ± 0.1)	19.0 ± 0.7 (7.0 ± 0.2)	−115

[a]Kinetic parameters were determined at pH 7.5. [b]Redox potentials determined by the xanthine oxidase method have a precision of ±5 mV. ND, not determined.

The pH profiles of the kinetic parameters for wild-type PutA and mutants D370A, E372A, and E373A were analyzed according to Dixon[15] and Cleland[16] for the effect of pH on enzyme−ligand complexes by plotting log k_{cat}, log k_{cat}/K_m, and pK_m vs pH. The associated pK_a values for the kinetic parameters were determined by best-fit analysis to eq 1 using Sigma Plot 12.0 Enzyme Kinetics, where P_{obs} and P_{lim} represent the observed and limiting parameter values, respectively, and pK_a is the acid dissociation constant of an ionizable group in the pH range studied.

$$P_{obs} = P_{lim}/(1 + 10^{(pK_a - pH)}) \quad (1)$$

Lipid Pull-Down and Functional Membrane Binding Assays. Lipid pull-down assays were performed similarly to that previously described.[11] In all assays, PutA proteins were incubated with 20 mM proline to reduce the bound FAD cofactor.

Functional membrane association activity of PutA was measured at 25 °C as described previously[9] by following the formation of a yellow complex between P5C and *o*-aminobenzaldehyde (*o*-AB) at 443 nm (ε = 2590 M^{-1} cm^{-1}) in a 96-well plate with 200 μL reaction volume for each assay. In addition to the assay buffer (50 mM MOPS, 10 mM $MgCl_2$, 10% glycerol, pH 7.4), the reaction mixture contained 4 mM *o*-AB, 60 mM proline, and 0.02 mg/mL of membrane vesicles prepared from *E. coli* strain JT31 *putA*$^-$. PutA (final concentration of 0.2 μM) was added to initiate the reaction. One unit of activity is the mass in milligrams of membrane vesicles that generates 1 μmole of the chromogenic complex per minute. Inverted *E. coli* strain JT31 *putA*$^-$ membrane vesicles were prepared as reported by Abrahamson et al., frozen in liquid N_2, and stored at −70 °C until needed.[17]

Determination of Flavin Redox Potentials. Reduction potentials were determined by the xanthine/xanthine oxidase method of Massey.[18] Resorufin (E_m = −79 mV) was used as the indicator dye. PutA proteins (25 μM) were mixed with 200 μM xanthine, 100 μM methyl viologen (mediator dye), and 10 μM resorufin in 50 mM potassium phosphate buffer (10% glycerol, 50 mM NaCl, pH 7.5). The protein mixture was degassed with nitrogen, and experiments were performed at 23 °C under anaerobic conditions in a nitrogen atmosphere in an anaerobic chamber (Belle Technology Glovebox). Reduction of PutA-bound FAD was initiated by adding 10 nM xanthine oxidase to the protein mixture and monitored by recording the UV−visible spectra using the scanning program of a Cary 100 UV−vis spectrophotometer.

Gel Mobility Shift Assays. The DNA binding affinity of the PutA mutant D370A was assessed by gel mobility shift assays as described using IRdye-700 (LI-COR, Inc.) 5′-end labeled *put* control DNA.[19]

Cell-Based Gene Expression Assay. *E. coli* strain JT31 *putA*$^-$ *lacZ*$^-$ containing *putC:lacZ* (pUT03) and various *putA* gene constructs (pUC18-PutA) were grown at 37 °C in minimal medium containing ampicillin (50 μg/mL) and chloramphenicol (30 μg/mL) to OD at 600 nm (OD_{600}) ∼ 1.0. Cells were then pelleted and immediately resuspended in ice-cold buffer Z (0.1 M sodium phosphate, 10 mM KCl, 1 mM $MgSO_4$, 50 mM β-mercaptoethanol, pH 7). In a separate 2 mL microcentrifuge tube, 10−50 μL of cell suspension was diluted to 1 mL with buffer Z, and then 100 μL of chloroform and 50 μL of 0.1% SDS were added. Samples were then vortexed and incubated in a water bath at 28 °C for 10 min. Next, 200 μL of *o*-nitrophenyl-β-D-galactopyranoside was added to each sample followed by vortexing and incubation at 28 °C. After 2−3 min of incubation, 500 μL of 1 M Na_2CO_3 was added to stop the reaction. Reaction mixtures were then spun (13 000 rpm, 5 min) with a benchtop centrifuge, and the OD at 420 (OD_{420}) and 550 nm (OD_{550}) of the supernatants were recorded with a Cary-100 UV−visible spectrophotometer along with the OD_{600} of the initial cell suspension. β-Galactosidase activity was then calculated as Miller units according to the method of Miller.[20] The results reported here are the average values from three independent experiments.

Crystallization of PRODH Domain Mutant Enzymes. Crystallization experiments were performed with site-directed mutants of PutA86−630 in which Asp370 is replaced with Ala (PutA86−630D370A) or Asn (PutA86−630D370N). These enzymes were expressed and purified using methods described previously for the PutA86−630 mutant Y540S.[21] PutA86−630D370A was purified using a single immobilized Ni^{2+} ion affinity chromatography step. Additional anion exchange (HiTrap Q) and gel filtration (Superdex 200) steps were used for PutA86−630D370N. The purified enzymes were dialyzed into 50 mM Tris-HCl buffer containing 20 mM NaCl, 0.5 mM EDTA, and 5% glycerol at pH 7.5, and concentrated

with centrifugal concentrators to 18 mg/mL (PutA86−630D370A) or 17 mg/mL (PutA86−630D370N) in preparation for crystallization trials. The protein concentration was estimated with the bicinchoninic acid method as implemented in a commercially available kit (Pierce). The C-terminal hexahistidine tag remained after purification.

Crystals of PutA86−630D370A and PutA86−630D370N complexed with the competitive inhibitor THFA were grown at room temperature in sitting drops using a protocol developed previously for the crystallization of PutA86−630 and the related PRODH domain construct PutA86−669.[14,21,22] Briefly, the enzyme at 16 mg/mL for PutA86−630D370A or 10 mg/mL for PutA86−630D370N was incubated with THFA (10 mM final concentration) prior to crystallization. The enzyme−inhibitor complex was then crystallized in sitting drops formed of equal volumes of the enzyme solution and a reservoir solution consisting of 11−26% (w/v) PEG 3350 and 0.1 M sodium citrate buffer in the pH range 5.5−5.9. In preparation for low-temperature data collection, the crystals were soaked in a cryobuffer containing 18% (w/v) PEG3350, 15% PEG200, and 0.1 M citrate buffer at pH 5.7, harvested with Hampton mounting loops, and plunged into liquid nitrogen.

X-ray Diffraction Data Collection, Processing, and Refinement. Diffraction data were collected at beamline 24-ID-C of the Advanced Photon Source. The space group is *I*222 with unit cell dimensions of a = 73 Å, b = 142 Å, and c = 147 Å, and one molecule in the asymmetric unit. We note that this crystal form is the same one used to determine the structure of the native EcPutA PRODH domain complexed with THFA.[14] The data set used for refinement of PutA86−630D370A−THFA consisted of 180 frames collected with oscillation width of 1° per frame and detector distance of 250 mm. The data set for PutA86−630D370N−THFA was collected similarly, except that the detector distance was 200 mm. The data were processed with HKL2000.[23] Data processing statistics are listed in Table 2.

Structure refinement calculations in PHENIX[24] were started from coordinates derived from the structure of the *E. coli* PutA PRODH domain complexed with THFA (PDB entry 1TIW)[14] by removing water and THFA and truncating Asp370 to Ala. Model building was done with Coot.[25] A common set of test reflections (5%) was used for both refinements, and this set corresponds to the one used previously for refinements of EcPutA PRODH domain structures.[8,13,14,21]

The final models for PutA86−630D370A−THFA and PutA86−630D370N−THFA each include one protein chain, one FAD cofactor, one THFA inhibitor, water molecules, and two PEG fragments (Table 2). As with all other structures of the EcPutA PRODH domain complexed with proline analogues,[8,13,14,21] electron density is strong for the $(\beta\alpha)_8$ barrel FAD-binding subdomain (residues 87−137, 259−612) and allowed for unambiguous modeling of this region of the structure. However, as observed previously, the density outside of this subdomain was significantly weaker implying substantial disorder. The final model for PutA86−630D370A−THFA includes residues 87−184, 204−215, 226−236, and 241−610. The model for PutA86−630D370N−THFA includes residues 87−187, 204−215, 226−236, and 242−610. The MolProbity scores for PutA86−630D370A−THFA and PutA86−630D370N−THFA are in 96th and 98th percentiles, respectively. The Ramachandran outliers lie on the edge of the α-helical region and correspond to residues in a helix−turn−helix region (residues 150−172) in the poorly ordered section of the structure.

Table 2. Data Collection and Refinement Statistics[a]

	PutA86−630D370A−THFA	PutA86−630D370N−THFA
space group	*I*222	*I*222
unit cell lengths (Å)	a = 73.3, b = 142.3, c = 146.6	a = 72.8, b = 140.5, c = 147.0
wavelength (Å)	0.97949	0.97949
diffraction resolution (Å)	50.0−1.90 (1.97−1.90)	50.0−1.85 (1.92−1.85)
no. of observations	448065	468660
no. of unique reflections	60923	64199
redundancy	7.4 (7.4)	7.3 (7.3)
completeness (%)	99.8 (100)	99.9 (100)
R_{merge} (I)	0.069 (0.419)	0.059 (0.417)
average I/σ	34.1 (3.4)	38.0 (4.2)
no. of protein chains	1	1
no. of protein atoms	3732	3728
no. of protein residues	491	493
no. of FAD atoms	53	53
no. of THFA atoms	8	8
no. of water molecules	214	258
no. of PEG atoms	26	26
R_{cryst}	0.190 (0.232)	0.192 (0.230)
R_{free}[b]	0.219 (0.291)	0.225 (0.296)
rmsd[c]		
bond lengths (Å)	0.007	0.007
bond angles (deg.)	1.06	1.08
Ramachandran plot[d]		
favored (%)	96.5	96.9
outliers (%)	0.8	0.6
average *B*-factors (Å^2)		
protein	44.1	37.4
FAD	26.1	21.4
THFA	29.2	25.7
water	39.9	36.5
PEG	66.0	60.3
coordinate error (Å)[e]	0.14	0.14
PDB accession code	4JNY	4JNZ

[a]Values for the outer resolution shell of data are given in parentheses. [b]5% common test set. [c]Compared to the Engh and Huber parameters.[28] [d]The Ramachandran plot was generated with RAMPAGE.[29] [e]Maximum likelihood-based coordinate error reported by PHENIX.

RESULTS

Kinetic Properties of PutA Mutants. Purified PutA mutants D370A, D370N, E372A, and E373A exhibited similar UV−visible spectra relative to wild-type PutA. The percent bound FAD was 66−80% per PutA polypeptide for the mutants compared to 80−85% for wild-type PutA. The steady-state kinetic parameters of PRODH activity (pH 7.5) for the mutants are summarized in Table 1. The changes in k_{cat} were modest with the D370N mutant about 3.5-fold lower and E373A

dx.doi.org/10.1021/bi400396g | *Biochemistry* 2013, 52, 4482−4491

slightly higher than wild-type PutA. The most significant change was observed in K_m and k_{cat}/K_m for the mutants D370A/N with k_{cat}/K_m values decreased by more than 10-fold relative to wild-type PutA. The mutant E372A results in a ~5-fold lower k_{cat}/K_m compared to wild-type PutA, whereas E373A exhibits no substantial change.

pH Profiles of PutA Mutants. Substitution of Asp/Glu residues with Ala (D370A, E372A, and E373A) may impact the pH profile of the PRODH reaction. Therefore, the pH dependence of the kinetic parameters k_{cat}, K_m, and k_{cat}/K_m of PRODH activity for wild-type PutA and mutants D370A, E372A, and E373A were determined. The pH dependence of k_{cat} (log scale) for each PutA protein is shown in Figure 2A and

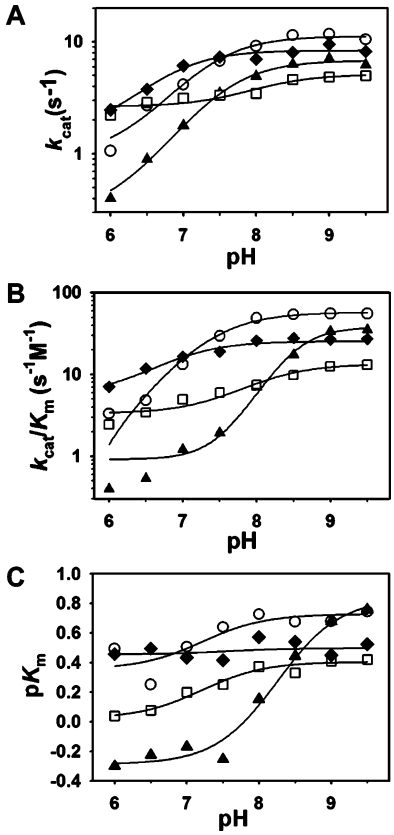

Figure 2. pH profiles of steady-state kinetic parameters of PutA wild-type and mutants. Measurements were performed in a 100 mM mixed buffer from pH 6–9.5 at 23 °C. (A) Plot of k_{cat} vs pH, (B) plot of k_{cat}/K_m vs pH, and (C) plot of pK_m for proline vs pH for PutA wild-type (○), D370A (▲), E372A (□), and E373A (♦). Best-fit analysis of the data to eq 1 yielded pK_a values as listed in Table 1.

is mostly similar for the different mutants with PRODH activity reaching a plateau above pH 8.0. Interestingly, the k_{cat} of E372A is least sensitive to pH changes. A pK_a of 7.3 was estimated for k_{cat} with wild-type PutA and with the different PutA mutants the pK_a values ranged from 6.8 to 8.1. The pH dependence of k_{cat}/K_m (Figure 2B) is similar for wild-type and E373A, but significant differences are observed with the other mutants, namely, D370A. A pK_a of 7.4 (k_{cat}/K_m) was estimated for wild-type PutA, whereas pK_a values of 8.1 and ~8.8 were determined for E372A and D370A, respectively. A plot of pK_m vs pH (Figure 2C) also shows a significant difference between PutA wild-type and D370A. The K_m values for proline for wild-type, E372A, and E373A are insensitive to pH at pH > 8, with estimated pK_a values ranging from 7.2 to 7.5. In contrast, D370A demonstrates a more than 6-fold decrease in K_m for proline at high pH with an estimated pK_a of 8.5 (Figure 2C).

Redox Properites of PutA Mutants. PutA-membrane binding is dependent on proline reduction of bound FAD, and thus changes in the redox potential of bound flavin would potentially impact PutA regulation. To explore this possibility, the flavin redox potentials of each PutA mutant were determined. The redox potentials (E_m) of PutA wild-type and mutants were estimated using the xanthine oxidase/dye method of Massey as shown in Figure 3 and summarized in Table 1.

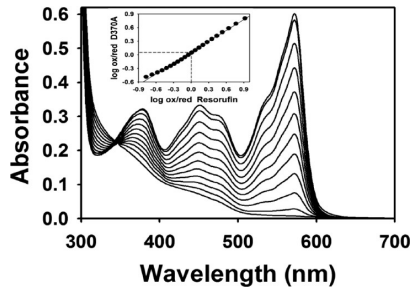

Figure 3. Redox potential determination of PutA mutant D370A at pH 7.5. D370A was mixed with 200 μM xanthine, 100 μM methyl viologen (mediator dye), and 10 μM resorufin (indicator dye) in 50 mM potassium phosphate buffer (10% glycerol and 50 mM NaCl). Reduction of the flavin cofactor was initiated by adding xanthine oxidase. A Nernst plot of oxidized/reduced flavin (D370A) versus oxidized/reduced resorufin is shown in the inset from which a redox potential of −81 mV (0.8 unit slope) was determined for D370A.

The estimated redox potentials for E372A and E373A deviated only slightly from wild-type PutA, whereas the E_m values for the D370A and D370N mutants were shifted about 25 mV more positive than wild-type PutA. These data show that in the different mutants reduction of the bound flavin by proline (E_m of −123 mV for the proline/P5C couple)[9] remains thermodynamically favorable. Also, the positive increase in redox poential observed for D370A and D370N is consistent with the fact that these mutations remove a negative charge near the isoalloxazine.

Lipid/Membrane Binding of PutA Mutants. The membrane binding properties of the PutA mutants were characterized by lipid pull-down assays as described previously for wild-type PutA.[11] In these assays, PutA is incubated with *E. coli* polar lipid vesicles in the absence and presence of proline, and the soluble and lipid-bound protein fractions are separated by centrifugation. In the absence of proline, the soluble/lipid distribution ratio (denoted $(S/L)_{ox}$) of wild-type, E372A, and E373A ranged from 4 to 8 indicating a strong preference for the soluble phase (Figure 4). In contrast, PutA mutants D370A/N showed a significant preference for the lipid fraction with D370A having $(S/L)_{ox}$ of 0.25. In control assays without lipids, D370A/N was in the soluble fraction indicating that D370A/N associated with lipids in the sedimentation experiments rather than associating with the walls of the tube.

The effect of proline was next assessed by incubating each protein with 20 mM proline in the presence of lipids. Prior to performing these assays, PutA mutants were titrated with proline to choose an optimal proline concentration for reducing the bound flavin cofactor in the lipid binding assays (Figure S1). Figure 4 shows that in the presence of proline, wild-type PutA and E373A appear primarily in the lipid-bound fraction

dx.doi.org/10.1021/bi400396g | *Biochemistry* 2013, 52, 4482–4491

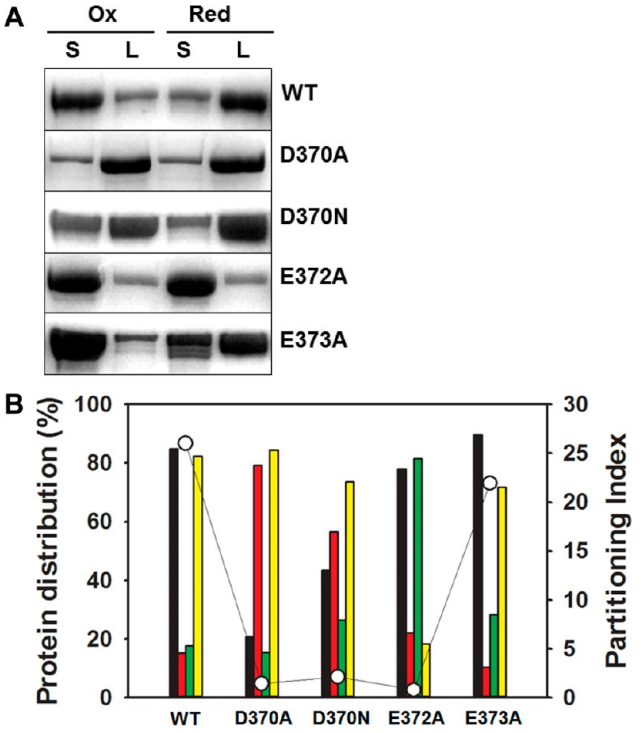

Figure 4. Lipid binding assays of PutA mutants. PutA wild-type and mutants (0.3 mg/mL) were incubated in HEPES buffer (pH 7.5, 150 mM NaCl) with freshly prepared *E. coli* polar lipids (0.8 mg/mL) for 1 h at room temperature in the absence or presence of 20 mM proline. (A) The soluble and lipid fractions were separated by Air-fuge ultracentrifugation, denatured with SDS buffer, and analyzed via SDS-PAGE. (B) Protein bands from SDS-PAGE were quantified using GelQuant.Net software, and the percent distribution of PutA in the soluble and lipid fractions were calculated for the oxidized and proline reduced samples. The results are shown as different colored bars (black, oxidized soluble; red, oxidized lipid; green, proline reduced soluble; yellow, proline reduced lipid). The open circles represent the partitioning index ($(S/L)_{ox}/(S/L)_{pro}$) which is a measure of the extent to which proline induces a change in the partitioning of PutA. Data shown are means ± standard errors from at least three experimental repeats.

with distribution ratios of $(S/L)_{pro}$ = 0.22 and $(S/L)_{pro}$ = 0.28, respectively, indicating proline-dependent partitioning from the soluble to lipid-bound form as previously shown for wild-type PutA.[11] The quantity $(S/L)_{ox}/(S/L)_{pro}$ is a measure of the extent to which proline induces a change in the partitioning of PutA. Large values of $(S/L)_{ox}/(S/L)_{pro}$ indicate that reduction of the flavin induces membrane binding of PutA. Such behavior is observed for wild-type and E373A (Figure 4B), which have $(S/L)_{ox}/(S/L)_{pro}$ of 25 and 20, respectively. On the other hand, for PutA mutants D370A, D370N, and E372A, no significant changes in partitioning were observed upon addition of proline (Figure 4B). D370A and D370N stayed predominatly in the lipid fraction, whereas E372A remained mostly in the soluble fraction regardless of the presence of proline indicating no significant increase in lipid binding.

To further explore the membrane interactions of the PutA mutants, functional membrane association assays were performed. In this assay, inverted membrane vesicles purified from a *putA*$^-$ mutant *E. coli* strain are used as the electron acceptor, and thus activity is dependent upon PutA forming an active complex with the membrane. Figure 5 shows that a severe loss in membrane functional activity is observed for

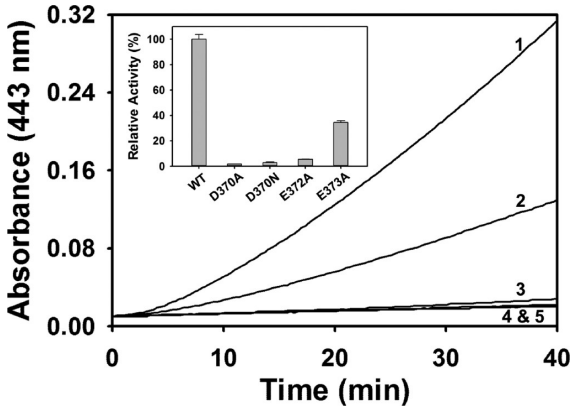

Figure 5. Functional membrane association assays. PutAs (0.2 μM) were incubated with 60 mM proline, 4 mM *o*-aminobenzaldehyde, and inverted membrane vesicles from *E. coli* strain JT31 *putA*$^-$ (0.02 mg/mL membrane protein) in 20 mM Mops buffer (pH 7.5) at 23 °C in a 96-well plate. The reactions were monitored at 443 nm to determine the membrane associated PRODH activity. The labeled traces 1, 2, 3, 4, and 5 are WT, E373A, E372A, D370A, and D370N, respectively. The calculated specific membrane binding activities for the corresponding PutAs in the above traces were 0.338, 0.121, 0.017, 0.006, and 0.010 units/mg of membrane protein, respectively. Inset: relative membrane binding activities of mutant PutAs compared to wild-type PutA. Data shown are means ± standard errors from at least three experimental repeats.

mutants D370A, D370N, and E372A, which exhibited >50-fold, >30-fold, and ~20-fold lower activity than wild-type PutA, respectively. The activity of the E373A mutant, however, decreased by only about 3-fold relative to wild-type (Figure 5). Thus, it appears that mutations D370A/N and E372A significantly perturb functional PutA membrane binding.

Cell-Based Assays of PutA Functional Switching. The impact of the glutamate cluster mutations on PutA functional switching was next examined by cell-based reporter assays. As previously reported for wild-type PutA, Figure 6 shows that the addition of proline to the cell culture medium increases β-galactosidase activity by 2.5-fold consistent with increased

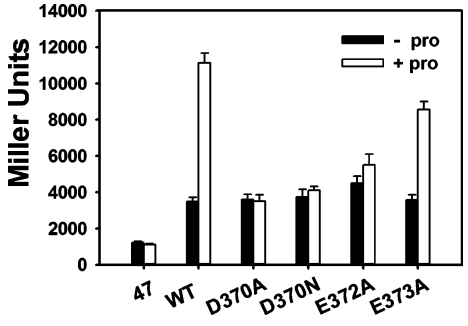

Figure 6. Cell-based functional switching assays of PutA wild-type and mutants. *E. coli* strain JT31 was grown in minimal medium at 37 °C in the absence or presence of 20 mM proline containing the low-copy *putC:lacZ* reporter construct and pUC18-PutA constructs expressing PutA wild-type, D370A, D370N, E372A, and E373A mutants. β-Galactosidase activity data are shown as the mean ± standard errors of three independent experiments. JT31 containing the *putC:lacZ* reporter construct and a pUC18 construct expressing PutA47 (contains first 47 residues of *E. coli* PutA) was used as a negative control. Data shown are means ± standard errors from at least three experimental repeats.

dx.doi.org/10.1021/bi400396g | *Biochemistry* 2013, 52, 4482−4491

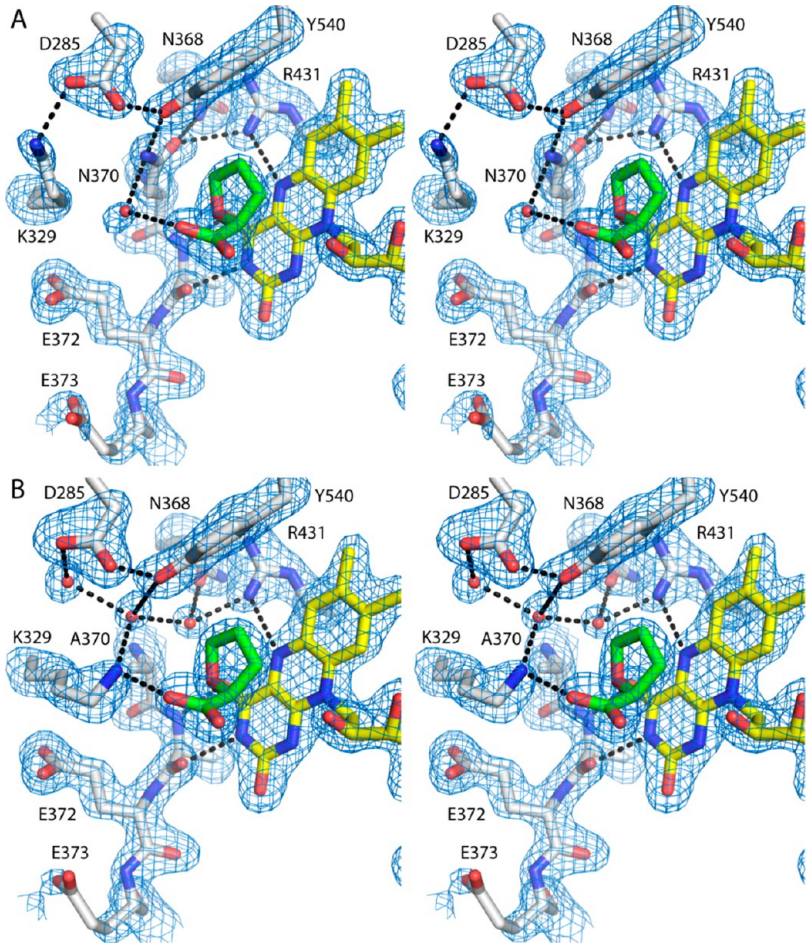

Figure 7. Stereographic view (relaxed) of the active sites of (A) PutA86−630D370N complexed with THFA and (B) PutA86−630D370A complexed with THFA. The cages represent simulated annealing σ_A-weighted $F_o - F_c$ maps contoured at 3σ. Prior to calculation of each map, FAD, THFA, the β3-α3 loop, and selected side chains and water molecules were omitted, and simulated annealing refinement was performed with PHENIX.

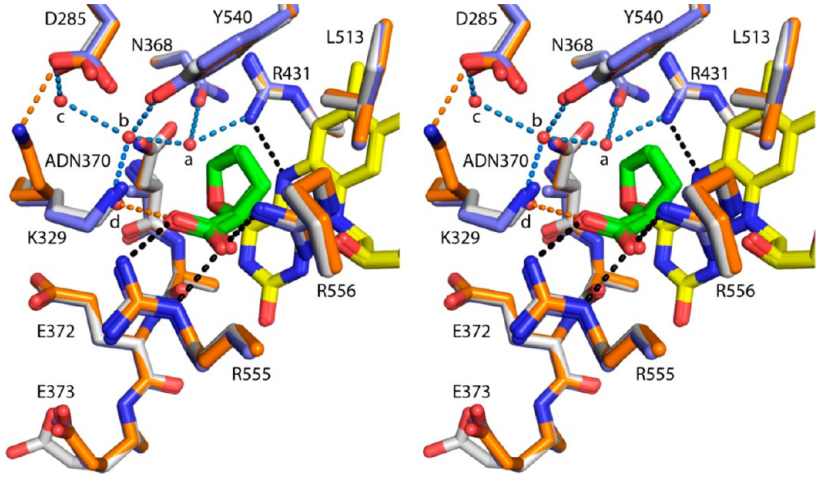

Figure 8. Stereographic view (relaxed) of a comparison of the active sites of PutA86−630D370N−THFA (orange), PutA86−630D370A−THFA (blue), and PutA86−669−THFA (white). Black dashed lines represent electrostatic interactions common to all three structures. Orange and blue dashed lines denote hydrogen bonds unique to the PutA86−630D370N and PutA86−630D370A structures, respectively. Water molecules unique to PutA86−630D370A are labeled a, b, and c. The letter d labels an active site water molecule unique to PutA86−630D370N.

proline relieving wild-type PutA repression of the *putC*:*lacZ* reporter gene.[4] PutA47, which is the N-terminal DNA-binding domain of PutA, strongly represses expression of the *lacZ* reporter gene in both the absence and presence of proline as expected (Figure 6). No apparent activation of *lacZ* gene expression was observed with PutA mutants D370A, D370N, and E372A in the presence of proline, suggesting that these mutants do not functionally switch *in vivo*. Cells expressing

dx.doi.org/10.1021/bi400396g | *Biochemistry* 2013, 52, 4482−4491

E373A, however, exhibited a 2-fold increase in β-galactosidase activity, which indicates proline-dependent regulation of E373A.

One plausible reason for the lack of proline-dependent activation of D370A/N and E372A in the cell-based assays is that these mutations may increase the binding affinity to the *put* control DNA. To test this possibility, DNA gel shift mobility assays of the D370A mutant with *put* control DNA were performed. A dissociation constant (K_D) of 31 ± 6 nM was determined for D370A (Figure S2), which is similar to that of wild-type PutA (K_D = 45 nM) suggesting no significant changes in DNA-binding affinity.[9]

Crystal Structures of PutA86−630D370A−THFA and PutA86−630D370N−THFA. The crystal structures of the PRODH domain with Asp370 mutated to either Asn or Ala were determined to characterize the structural perturbations caused by these mutations (Table 2). As expected, the mutant enzymes display the distorted $(\beta\alpha)_8$ fold that is characteristic of the PRODH family (Figure 1A).[1] The root-mean-square deviations between the mutant enzymes and the native PRODH domain (PDB 1TIW) are less than 0.4 Å (493−496 aligned residues), indicating that mutation of Asp370 causes no significant change in the global structure of the PRODH domain.

Electron density maps clearly indicated the locations of the FAD cofactor, bound THFA ligand, and active site residues (Figure 7). The FAD conformation is identical to that of the native enzyme. Also, the location of THFA centered over the middle ring of the isoalloxazine ring system is also seen in the native enzyme. Most of the noncovalent interactions of the inhibitor are identical to those of the native enzyme complex, including the ion pairing of the inhibitor carboxylate with Arg555 and Arg556, the nonpolar interactions involving Leu513, Tyr540, and Tyr552, and the water-mediated hydrogen bond between the THFA heteroatom and Tyr437. Thus, the structures show that the mutated enzymes bind THFA, and by inference proline, in essentially the same manner as the native enzyme.

Although the structures of the mutant and native enzymes are very similar, the mutations do induce small structural changes in the local environment of residue 370 (Figure 8). Mutation of Asp370 to Asn induces rotation of Lys329 away from the THFA carboxylate and toward Asp285. This conformational change apparently avoids the unfavorable juxtaposition of two hydrogen bond donors — the ε-amino of Lys329 and the side chain amino group of Asn370 — that would have occurred had Lys329 adopted the conformation found in the native enzyme. Note that a water molecule fills the spot vacated by the ε-amino of Lys329 (labeled d in Figure 8). On the other hand, mutation of Asp370 to Ala primarily changes the solvent structure of the active site. Two new water molecules have entered the active site and occupy the space of the eliminated carboxylate (labeled a and b in Figure 8). These water molecules serve the same roles as the oxygen atoms of the carboxylate of Asp370 by interacting with Arg431, Lys329, Tyr540, and Asn368. The D370A mutation also causes a subtle deflection of Asp285, which allows enough space for a third new water molecule to enter the active site (labeled c in Figure 8).

Finally, mutation of Asp370 to either Asn or Ala appears to induce disorder in Glu373. The electron density for this residue is quite strong in the native PRODH domain structure and indicates that Glu373 adopts a single conformation as shown in Figure 8. Density for the side chain of Glu373 is diffuse in the two mutant enzyme structures (Figure 7), suggesting that the side chain exhibits substantial disorder.

DISCUSSION

Comparison of the crystal structures of the PRODH domain (PutA86−630) complexed with THFA and inactivated with PPG suggested that the different positions occupied by Asp370 (Figure 1B) are dependent on the redox state of the flavin. Additionally, interactions between Asp370 and Glu372 identified in the structure of PPG-inactivated PutA86−630 indicated a potential molecular pathway for mediating redox changes beyond the inner sphere of the active site. Residues Asp370, Glu372, and Glu373 are highly conserved in PutAs, suggesting they have important roles in PRODH domain structure and function. Therefore, the carboxylate functionality of Asp370, Glu372, and Glu373 was removed to test this possible pathway in PutA functional switching.

Removal of active site ionizable groups such as Asp370 are anticipated to influence the pH dependence of activity. The pH profile of k_{cat} shows that deprotonation of a group on the E−S complex, which is important for catalysis, occurs in PutA wild-type and mutants. At high pH, k_{cat} values only vary by 2-fold for wild-type and PutA mutants, suggesting that Asp370, Glu372, and Glu373 are not critically involved in a catalytic step. The pH profile of D370A was altered the most significantly with a > 1.6 unit increase in the pK_a of k_{cat}/K_m and K_m relative to wild-type PutA. The difference in the pH dependence of k_{cat}/K_m between PutA wild-type and the D370A mutant reflects the ionization of a group on the enzyme or substrate. A critical step in the PRODH reaction is deprotonation of the proline amine group.[26] We note that one of the side chain O atoms of Asp370 is 4.0 Å from the O heteroatom atom of THFA, which represents the amine of proline. Also, in the THFA complex, Asp370 forms an ion pair (3.1 Å) with the ε-amino group of Lys329 that has been shown to form a covalent link with the mechanism based inhibitor *N*-propargylglycine.[11] Thus, Asp370 is positioned to influence different ionizable groups in the PutA active site. In the first crystal structure of the PRODH domain of *E. coli*, Asp370 was identified as an important active site residue involved in hydrogen bonding interactions with Tyr540 and Arg431.[13] The impact of replacing D370 with Ala on the steady-state kinetic parameters was previously investigated in a PRODH domain construct of *E. coli* (PutA86−630D370A).[26] Although the increase was not as dramatic, the pK_a of k_{cat}/K_m for PutA86−601D370A was 0.8 units higher than wild-type PutA86−601 consistent with the results here for full-length PutA.[26]

A significant defect in PutA functional switching was observed with the PutA mutants D370A and D370N. These mutants associated with the lipids in the absence and presence of proline and showed no evidence of functional switching. The lipid binding of D370A and D370N appears to be nonspecific as the functional membrane association activities of these mutants were 50- and 30-fold lower than wild-type PutA, respectively. The crystal structure of PutA86−630D370A−THFA and PutA86−630D370N−THFA shows that mutation of Asp370 does not cause significant changes in the β3-α3 loop region or in the global structure of the PRODH domain. Thus, the functional consequences observed with the PutA D370A and D370N mutants are most likely due to impaired flavin redox signaling to regions beyond the PRODH active site,

dx.doi.org/10.1021/bi400396g | *Biochemistry* 2013, 52, 4482−4491

rather than intrinsic conformational defects in the PRODH domain.

The PutA mutant E372A was also shown to be defective in lipid binding, but it was found predominantly in the soluble fraction in the absence and presence of proline. E372A exhibited significantly lower functional membrane association activity despite having only a slight decrease in proline:DCPIP oxidoreductase activity relative to wild-type PutA (Table 1). These results show that removal of the carboxylate group of Asp370 or Glu372, or replacement of Asp370 with the nonionizable asparagine, results in dysfunctional PutA membrane associations and indicates that these charged residues on the β3-α3 loop are important for regulation of PutA functional membrane binding. Consistent with the *in vitro* membrane binding studies, cell-based assays using a *lacZ* reporter gene also showed that D370A/N and E372A do not respond to proline like the wild type enzyme. Thus, both membrane binding and cell based transcriptional activation assays show that Asp370 and Glu372 have important roles in regulating PutA function.

In contrast to Asp370 and Glu372, removal of Glu373 had only minor effects on membrane binding. Similar to wild-type PutA, E373A strongly partitions into the lipid fraction in the presence of proline and has membrane functional activity that is only 3-fold lower than wild-type PutA. In the *lacZ* reporter assays, E373A also showed increased β-galactosidase activity with proline, which is similar to wild-type PutA and consistent with allosteric regulation of PutA by proline in the cell.

In studies of PutA functional switching, it can be challenging to distinguish between the catalytic and regulatory roles of a particular active site residue because flavin reduction is a requisite step for activation of membrane binding. Glu372 is a notable exception. The E372A mutation minimally affects PRODH activity but significantly impacts both the membrane binding activity and the transcriptional activation response to proline in cell-based assays. Thus, while Glu372 seems to have only a minor part in catalysis, it clearly plays a significant role in functional switching.

The results from this study strongly point to the β3-α3 loop being involved in the signaling mechanism of PutA and suggest that conformational changes of Glu372 and Asp370 are part of the larger, global structural change that drives membrane binding. In the oxidized enzyme, Asp370 interacts with Asp368 and Arg431, while Glu372 forms two hydrogen bonds with Ser331 of the adjacent β2-α2 loop (Figure 1B). Reduction of the flavin via PPG inactivation induces rotations of both residues, which breaks three of the four interactions and creates a new hydrogen bond between Asp370 and the backbone of Leu330 of the β2-α2 loop. Furthermore, Asp370 and Glu372 form an unfavorable electrostatic interaction in the reduced state. How this rearrangement of noncovalent interactions within the active site affects PutA membrane binding is not obvious. One possibility is that they encourage Arg431 to disengage from the N5 of the flavin, which promotes the observed bending of the isoalloxazine and perhaps additional global conformational changes to occur; these additional protein conformational changes are not evident from the truncated domain construct used for crystallography.

Another explanation is that the charged residues on the β3-α3 loop act through a less specific electrostatic effect. The carboxylate groups of Asp370, Glu372, and Glu372 are poised 5 Å, 10 Å, and 14 Å, respectively, from the flavin N5 atom. Reduction of the FAD presumably results in electrostatic repulsion between these side chains and the reduced isoalloxazine. This Coulombic repulsion may be a source of activation energy that drives the conformational changes that underlie functional switching. Interestingly, the degree of impairment of functional switching caused by the mutations varies inversely with the distance from the isoalloxazine (Figures 5 and 6), with mutation of Asp370 having the greatest effect, followed by Glu372, and mutation of Glu373 having a negligible effect on switching. This observation is consistent with an electrostatic effect. An analogous idea involving a glutamate residue near the flavin has been proposed to explain substrate selectivity in the flavoenzymes fumarate reductase and succinate oxidase.[27] Future studies will thus seek to build molecular links from the β3-α3 loop region to the membrane association domain of PutA.

■ ASSOCIATED CONTENT

Ⓢ Supporting Information

Figures S1 and S2 are available free of charge via the Internet at http://pubs.acs.org.

Accession Codes

Coordinates and structure factors have been deposited in the Protein Data Bank under accession numbers 4JNY and 4JNZ.

■ AUTHOR INFORMATION

Corresponding Author

*Tel: 402-472-9652. Fax: 402-472-7842. E-mail: dbecker3@unl.edu.

Funding

This research was supported by NIH GM061068 and is a contribution of the University of Nebraska Agricultural Research Division, supported in part by funds provided through the Hatch Act. This publication was also made possible by NIH Grants P20 RR-017675 and P30GM103335 and NSF Grant DBI-0851747.

Notes

The authors declare no competing financial interest.

■ ACKNOWLEDGMENTS

We thank Dr. Jonathan Schuermann for help with X-ray data collection and processing. This work is based upon research conducted at the Advanced Photon Source on the Northeastern Collaborative Access Team beamlines, which are supported by grants from the National Center for Research Resources (5P41RR015301-10) and the National Institute of General Medical Sciences (8 P41 GM103403-10) from the National Institutes of Health. Use of the Advanced Photon Source, an Office of Science User Facility operated for the U.S. Department of Energy (DOE) Office of Science by Argonne National Laboratory, was supported by the U.S. DOE under Contract No. DE-AC02-06CH11357.

■ ABBREVIATIONS

DCPIP, dichlorophenolindophenol; D370A, site-directed mutant of EcPutA in which Asp370 is replaced with Ala; D370N, site-directed mutant of EcPutA in which Asp370 is replaced with Asn; E372A, site-directed mutant of EcPutA in which Glu372 is replaced with Ala; E373A, site-directed mutant of EcPutA in which Glu373 is replaced with Ala; EcPutA, proline utilization A from *Escherichia coli*; FAD, flavin adenine dinucleotide; GSA, γ-glutamate semialdehyde; HEPES, *N*-(2-hydroxyethyl)piperazine-*N*′-2-ethanesulfonic acid; MOPS, 3-(*N*-morpholino)propanesulfonic acid; *o*-AB, *o*-aminobenzalde-

hyde; PRODH, proline dehydrogenase; P5C, Δ^1-pyrroline-5-carboxylate; P5CDH, Δ^1-pyrroline-5-carboxylate dehydrogenase; PutA, proline utilization A; PutA86−630, protein corresponding to residues 86−630 of *E. coli* PutA; PutA86−630D370A, site-directed mutant of PutA86−630 in which Asp370 is replaced with Ala; PutA86−630D370N, site-directed mutant of PutA86−630 in which Asp370 is replaced with Asn; PutA86−669, protein corresponding to residues 86−669 of *E. coli* PutA; SDS, sodium dodecyl sulfate; THFA, L-tetrahydro-2-furoic acid

REFERENCES

(1) Tanner, J. J. (2008) Structural biology of proline catabolism. *Amino Acids 35*, 719−730.

(2) Menzel, R., and Roth, J. (1981) Enzymatic properties of the purified PutA protein from *Salmonella typhimurium*. *J. Biol. Chem. 256*, 9762−9766.

(3) Moxley, M. A., Tanner, J. J., and Becker, D. F. (2011) Steady-state kinetic mechanism of the proline:ubiquinone oxidoreductase activity of proline utilization A (PutA) from *Escherichia coli*. *Arch. Biochem. Biophys. 516*, 113−120.

(4) Zhou, Y., Larson, J. D., Bottoms, C. A., Arturo, E. C., Henzl, M. T., Jenkins, J. L., Nix, J. C., Becker, D. F., and Tanner, J. J. (2008) Structural basis of the transcriptional regulation of the proline utilization regulon by multifunctional PutA. *J. Mol. Biol. 381*, 174−188.

(5) Zhang, W., Zhou, Y., and Becker, D. F. (2004) Regulation of PutA-membrane associations by flavin adenine dinucleotide reduction. *Biochemistry 43*, 13165−13174.

(6) Wood, J. M. (1987) Membrane association of proline dehydrogenase in *Escherichia coli* is redox dependent. *Proc. Natl. Acad. Sci. U. S. A. 84*, 373−377.

(7) Ostrovsky de Spicer, P., and Maloy, S. (1993) PutA protein, a membrane-associated flavin dehydrogenase, acts as a redox-dependent transcriptional regulator. *Proc. Natl. Acad. Sci. U. S. A. 90*, 4295−4298.

(8) Zhang, W., Zhang, M., Zhu, W., Zhou, Y., Wanduragala, S., Rewinkel, D., Tanner, J. J., and Becker, D. F. (2007) Redox-induced changes in flavin structure and roles of flavin N(5) and the ribityl 2'-OH group in regulating PutA-membrane binding. *Biochemistry 46*, 483−491.

(9) Becker, D. F., and Thomas, E. A. (2001) Redox properties of the PutA protein from *Escherichia coli* and the influence of the flavin redox state on PutA-DNA interactions. *Biochemistry 40*, 4714−4721.

(10) Zhu, W., and Becker, D. F. (2003) Flavin redox state triggers conformational changes in the PutA protein from *Escherichia coli*. *Biochemistry 42*, 5469−5477.

(11) Srivastava, D., Zhu, W., Johnson, W. H., Jr., Whitman, C. P., Becker, D. F., and Tanner, J. J. (2010) The structure of the proline utilization a proline dehydrogenase domain inactivated by N-propargylglycine provides insight into conformational changes induced by substrate binding and flavin reduction. *Biochemistry 49*, 560−569.

(12) White, T. A., Krishnan, N., Becker, D. F., and Tanner, J. J. (2007) Structure and kinetics of monofunctional proline dehydrogenase from *Thermus thermophilus*. *J. Biol. Chem. 282*, 14316−14327.

(13) Lee, Y. H., Nadaraia, S., Gu, D., Becker, D. F., and Tanner, J. J. (2003) Structure of the proline dehydrogenase domain of the multifunctional PutA flavoprotein. *Nat. Struct. Biol. 10*, 109−114.

(14) Zhang, M., White, T. A., Schuermann, J. P., Baban, B. A., Becker, D. F., and Tanner, J. J. (2004) Structures of the *Escherichia coli* PutA proline dehydrogenase domain in complex with competitive inhibitors. *Biochemistry 43*, 12539−12548.

(15) Dixon, M. (1953) The effect of pH on the affinities of enzymes for substrates and inhibitors. *Biochem. J. 55*, 161−170.

(16) Cleland, W. W. (1982) The use of pH studies to determine chemical mechanisms of enzyme-catalyzed reactions. *Methods Enzymol. 87*, 390−405.

(17) Abrahamson, J. L., Baker, L. G., Stephenson, J. T., and Wood, J. M. (1983) Proline dehydrogenase from *Escherichia coli* K12. Properties of the membrane-associated enzyme. *Eur. J. Biochem. 134*, 77−82.

(18) Massey, V. (1991) A simple method for the detemination of redox potentials, In *Flavins and Flavoproteins* (Curti, B., Ronchi, S., and Zanetti, G., Eds.) pp 59−66, Walter de Gruyter and Company, Berlin.

(19) Gu, D., Zhou, Y., Kallhoff, V., Baban, B., Tanner, J. J., and Becker, D. F. (2004) Identification and characterization of the DNA-binding domain of the multifunctional PutA flavoenzyme. *J. Biol. Chem. 279*, 31171−31176.

(20) Miller, J. H. (1972) *Experiments in Molecular Genetics*, Cold Spring Harbor Laboratory, Cold Spring Harbor, NY.

(21) Ostrander, E. L., Larson, J. D., Schuermann, J. P., and Tanner, J. J. (2009) A conserved active site tyrosine residue of proline dehydrogenase helps enforce the preference for proline over hydroxyproline as the substrate. *Biochemistry 48*, 951−959.

(22) Nadaraia, S., Lee, Y. H., Becker, D. F., and Tanner, J. J. (2001) Crystallization and preliminary crystallographic analysis of the proline dehydrogenase domain of the multifunctional PutA flavoprotein from *Escherichia coli*. *Acta Crystallogr. D57*, 1925−1927.

(23) Otwinowski, Z., and Minor, W. (1997) Processing of X-ray diffraction data collected in oscillation mode. *Methods Enzymol. 276*, 307−326.

(24) Zwart, P. H., Afonine, P. V., Grosse-Kunstleve, R. W., Hung, L. W., Ioerger, T. R., McCoy, A. J., McKee, E., Moriarty, N. W., Read, R. J., Sacchettini, J. C., Sauter, N. K., Storoni, L. C., Terwilliger, T. C., and Adams, P. D. (2008) Automated structure solution with the PHENIX suite. *Methods Mol. Biol. 426*, 419−435.

(25) Emsley, P., and Cowtan, K. (2004) Coot: model-building tools for molecular graphics. *Acta Crystallogr. D60*, 2126−2132.

(26) Baban, B. A., Vinod, M. P., Tanner, J. J., and Becker, D. F. (2004) Probing a hydrogen bond pair and the FAD redox properties in the proline dehydrogenase domain of *Escherichia coli* PutA. *Biochim. Biophys. Acta 1701*, 49−59.

(27) Maklashina, E., Iverson, T. M., Sher, Y., Kotlyar, V., Andrell, J., Mirza, O., Hudson, J. M., Armstrong, F. A., Rothery, R. A., Weiner, J. H., and Cecchini, G. (2006) Fumarate reductase and succinate oxidase activity of *Escherichia coli* complex II homologs are perturbed differently by mutation of the flavin binding domain. *J. Biol. Chem. 281*, 11357−11365.

(28) Engh, R. A., and Huber, R. (1991) Accurate bond and angle parameters for x-ray protein structure refinement. *Acta Crystallogr. A47*, 392−400.

(29) Lovell, S. C., Davis, I. W., Arendall, W. B., 3rd, de Bakker, P. I., Word, J. M., Prisant, M. G., Richardson, J. S., and Richardson, D. C. (2003) Structure validation by Calpha geometry: phi,psi and Cbeta deviation. *Proteins 50*, 437−450.

(30) DeLano, W. L. (2002) *The PyMOL User's Manual*, DeLano Scientific, San Carlos, CA.